



CFD ANALYSIS OF AN EJECTOR FOR COOLING APPLICATIONS

Shivakumar V¹, Patti Shiva², Dr. Sampath Rao³

¹Anurag Group of Institutions (Formerly CVSR College Of Engineering) (Autonomous),
Hyderabad

^{2,3}Vijay Rural Engineering College, Nizamabad

Abstract

Vapor-jet ejectors have been used in cooling/refrigeration applications since the early 1900s. Recent efforts to reduce energy consumption by harnessing energy from low grade industrial waste heat or renewable energy sources have resulted in a renewed interest in this technology. This project presents the results of computational fluid dynamics (CFD) simulations of a vapor-jet ejector operating with R134a as the working fluid. The impact of varying operating conditions on ejector performance is presented. Also considered in this study is the impact of varying three geometrical parameters on ejector performance: the mixing section length and radius, and the primary nozzle exit radius (representative of the velocity of the motive stream). The results of this study show that CFD is a useful tool in the design and optimization of ejectors for refrigeration devices.

KEYWORDS: Vapor-jet ejectors, CFD, R245fa, mixing section length and radius, primary nozzle, refrigeration devices.

I. INTRODUCTION

Ejector having convergent and divergent section as shown in figure 1.1. It is used to convert pressure energy of steam to kinetic energy. The cooling ejectors offer a simple, reliable, low-cost way to produce vacuum. They are especially effective in the chemical industry where an on-site supply of the high-pressure motive gas is available.

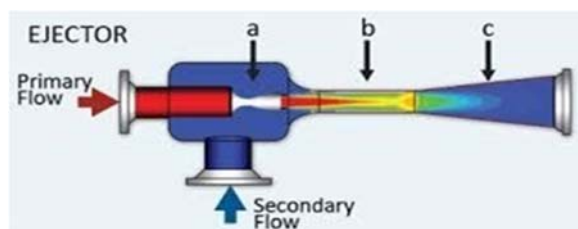


Figure 1.1 Ejector

The ejector cycle is best characterized by the entrainment ratio and the critical condenser pressure. The entrainment ratio (ω) is defined as the ratio of the primary mass flow rate that comes from the generator to the secondary mass flow rate that comes through the evaporator. In a feature unique to supersonic vapour-jet ejectors, the entrainment ratio of the ejector is constant over a wide range of condenser pressures.

II. METHODOLOGY

2.1 MODELING OF THE PROBLEM

A schematic drawing of a vapour-jet ejector that shows the characteristic dimensions used in this study is shown in Figure 2.1. It has been assumed that the ejector is axi-symmetric along the z-axis, thus only a thin slice of an ejector is modeled. Essentially, the ejector consists of two annular converging-diverging nozzles. In the outer nozzle, gas from the evaporator enters axially into the space outside the primary nozzle. Along 12, the secondary flow is accelerated until it mixes with the primary flow in 13. Along 14, the mixed flow is expanded through the diffuser until it exits the ejector. The primary flow from the generator enters and is compressed along 15 until it reaches the throat, at which point the flow is choked. Along

16, the primary flow is expanded to supersonic speeds.

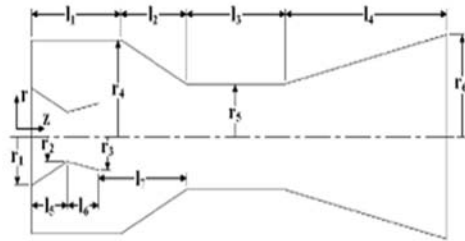


Figure 2.1 Typical ejector geometry used in CFD model.

	L₂	L₃	L₄	L₅	L₆	L₇
	27.0	36.0	37.36	85.78	17.0	10.0
	R₁	R₂	R₃	R₄	R₅	R₆
	3.0	1.48	2.35	15.0	4.5	12.14

Table 2.1 Shows That Geometric Of The Base Ejector Used In The Present (All Dimensions In mm)

2.2 GOVERNING EQUATIONS

The flows in the presented vapour-jet ejectors model are considered to be compressible, steady-stated, two dimensional and axis-symmetric. The model was written using the commercial CFD code PHOENICS V3.5.1. Under steady-state conditions, the general form of the governing equations, neglecting time derivative

Specific definitions of the variables ϕ , $\Gamma\phi$ and $S\phi$ for the cases of the continuity, momentum and energy equations are provided in Table 2.1

Equation	ϕ	Γ_ϕ	S_ϕ
Continuity	1	0	0
z-momentum	w	$\rho(v_r + v_\theta)$	$-\frac{\partial p}{\partial z} + \text{gravity} + \text{friction}...$
r-momentum	v	$\rho(v_r + v_\theta)$	$-\frac{\partial p}{\partial r} + \text{gravity} + \text{friction}...$
energy	h	$\rho \left(\frac{v_r}{Pr} + \frac{v_\theta}{PrL} \right)$	$-\frac{Dp}{Dt} + \text{heat sources} + ...$

Table 2.1 Continuity, Momentum and Energy equations.

2.3 DESIGNING OF EJECTOR

Figures 2.2, 2.3 and 2.4 are design of ejector using NX 8.0

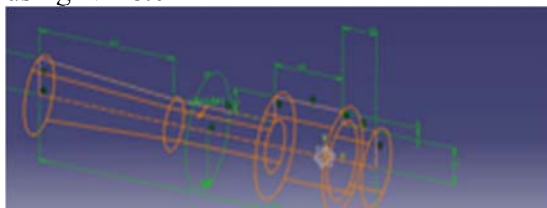


Fig 2.2 Wire Mesh Model of Ejector Body With Dimensions.



Figure 2.3 Isometric View of Ejector Body.

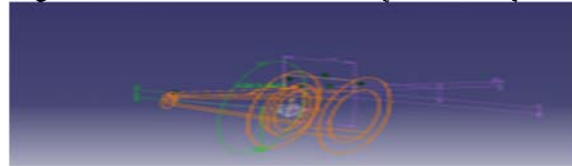


Fig 2.4 Wire Mesh Model of Motive Nozzle.

2.5 MESHING

The Figure shown 2.5 is the meshed model of rigid flange coupling in the ANSYS analysis for the static structural process. To analyse, the FEM triangular type of mesh is used for the rigid flange coupling in the ANSYS environment. The number of elements used in this meshing is 71441 and the number of nodes is 122228. In this process regular type of meshing is done to analyse the process.

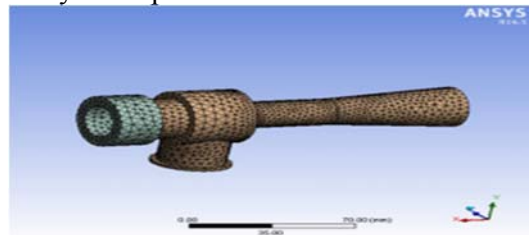


Figure 2.5 Meshing Model of Ejector

III. RESULTS AND DISCUSSIONS

The CFD model was initially used to verify the performance of single ejector geometry, operating with R245fa, over a wide range of operating temperatures. The generator temperature ranged from 60°C to 120°C in 20°C increments, the evaporator temperature ranged from -10°C to 20°C in increments of 5°C. A summary of these results showing only the critical point is presented in Fig. 5. The critical point for the ejector is shown the value of the entrainment ratio at the critical condenser pressure where, for the purposes of this study, the critical condenser pressure was defined as the condenser pressure at which the entrainment ratio was reduced to 95 % of the critical operation value.

Figure 3.1 shows critical condenser pressure verse entrainment ratio.

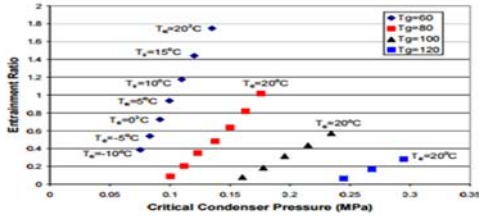


Figure 3.1 Shows Critical Condenser Pressure Verse Entrainment Ratio
3.1 CFD ANALYSIS ON EJECTOR ORIGINAL MODEL (Working fluid R134a)

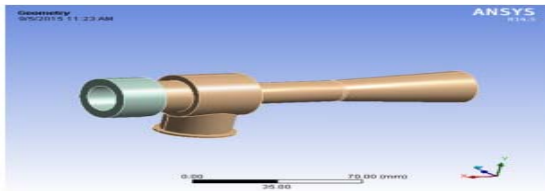


Figure 3.2 Geometric Model

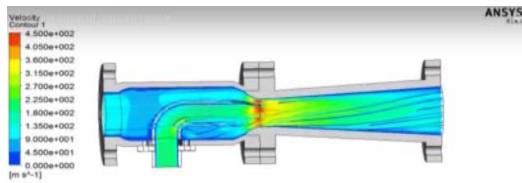


Figure 3.3 Velocity Counter1

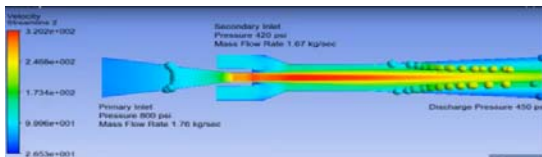


Fig 3.4 Velocity Steam Line 2

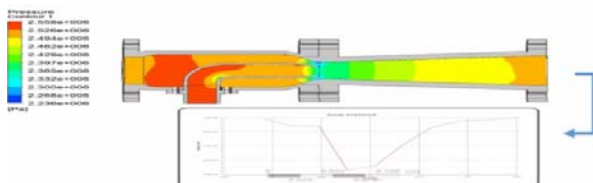


Figure 3.5 Pressure Counter1 Minimum Deformation

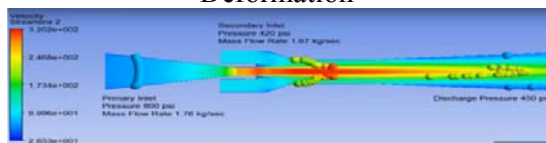


Figure 3.6 Secondary Inlet Pressure



Figure 3.7 Explaining Wall Shear Stress

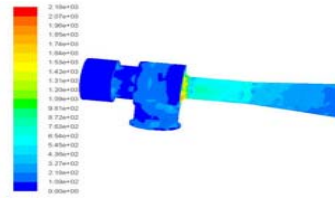


Figure 3.8 Explaining Turbulent Kinetic Energy

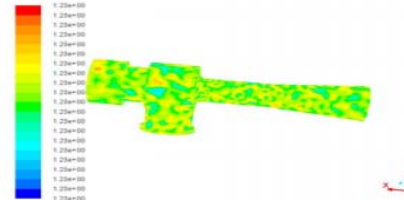


Figure 3.9 Explaining Density

3.2 CFD ANALYSIS ON EJECTOR MODIFIED 1(Working fluid R134a)

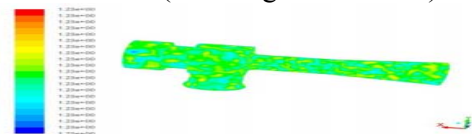


Fig 3.10 Mass Flow Rate Results

3.3 CFD ANALYSIS ON EJECTOR MODIFIED 2 (Working fluid R134a)

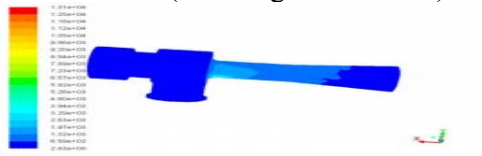


Figure 3.11 Explaining Turbulent Kinetic Energy

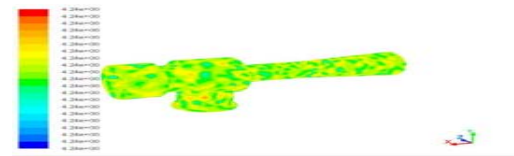
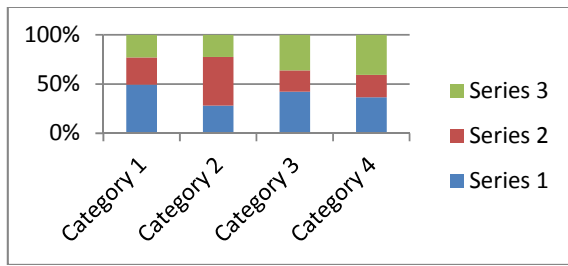


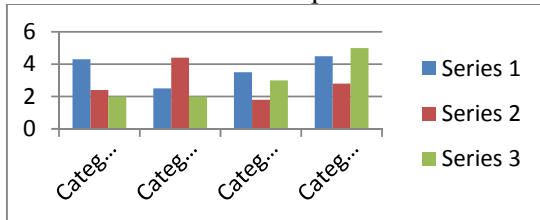
Fig 3.12 Explaining Density

Table 3.1 CFD Analysis Of Ejector Results

	VELOCITY MAGNITUDE	STATIC PRESSURE		
		max	min	
original	6.72E+02	-2.77E+05	2.07E+03	3.00E+02
Modified 1	1.76E+01	-1.92E+02	1.03E+02	3.00E+02
Modified 2	1.74E+02	-2.93E+03	1.01E+03	3.00E+02



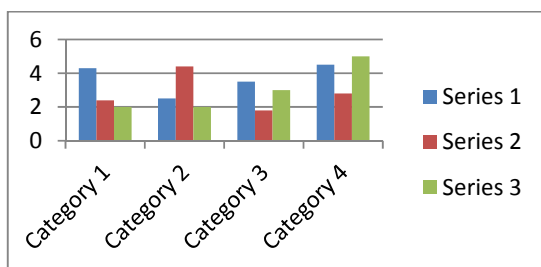
Graph 3.1 Shows There Is No Change In The Static Temperature.



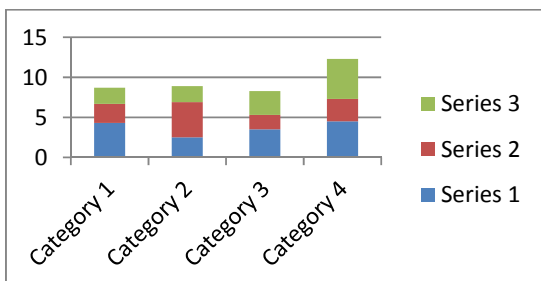
Graph 3.2 Velocity Magnitude

Table 3.2 CFD Analysis of Ejector Results

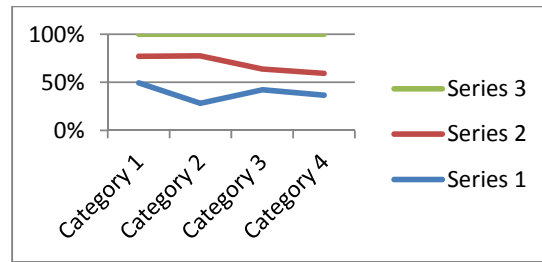
	SHEAR STRESS	KINETIC ENERGY		DENSITY	MASS FLOW RATE
		max	min		
original	2.18E+03	2.43E+001	1.31E+04	1.23E+00	6.24E-06
Modified 1	4.96E+00	1.00E-03	1.71E+01	1.23E+00	1.86E-06
Modified 2	0	2.43E+00	1.31E+04	4.24E+00.9	0.925E-03



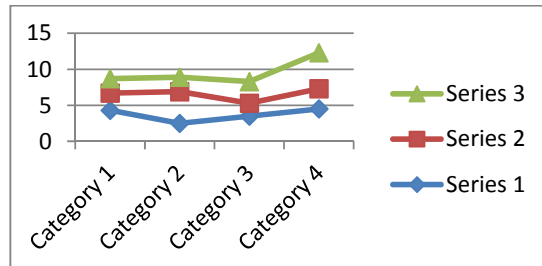
3.3 Graph Kinetic Energy



Graph 3.4 Density



Graph 3.5 Mass Flow Rate



Graph 3.6 Shows That Geometric of The Base Ejector Used In The Present (All Dimensions In mm)

IV. CONCLUSION

In this paper we have designed a ejector with geometrical parameter it is different throat radius, at the nozzle will be considered. And the analysis in computational fluid dynamics (CFD) simulations of a vapor-jet ejector operating with R134a as the working fluid will be analyzed. The impact of varying geometrical parameter such as throat radius on ejector performance is considered. As we compare the results obtained for the 3 types of analysis graphs and tables we can observe that the stress is very less an even negligible for the 2nd modified model, mass flow rates increase in the 2nd modified model and even if we see the remaining results we can conclude that the ejector with the diameter of throat inlet 3mm is a better product with best material by using R134a. Ejector systems support vacuum tower operation. Proper operation of an ejector system is important; without it, the vacuum tower performance is not optimal. When tower pressure increases above design operating pressure, flash zone pressure increases proportionally. The consequence of higher flash zone pressure is reduced vacuum gas oil yields and increased vacuum resid. When charge rates to the tower are less than design, the ejector system will pull the tower to a lower pressure. Lower pressure in the tower may adversely affect tower hydraulics and cause flooding. This will affect vacuum gas oil quality. With annual performance evaluations of

ejector systems, improved product quality, increased unit throughput or reductions in operating costs can often be realized.

REFERENCES

1. Alizadeh, S., Bahar, F., Geoola, F., Design and optimization of an absorption refrigeration system operated by solar energy, *Solar Energy*, Vol. 22, (1997), pp. 149-154
2. Anand, D.K., Kumar, B., Absorption machine irreversibility using new entropy calculations, *Solar Energy*, Vol.39, (1987), pp. 243-256
3. Tyagi, K.P., Design parameters of an aqua-ammonia vapour absorption refrigeration system, *Heat recovery systems & CHP*, Vol. 8(4), (1988), pp. 375- 377
4. ErcanAtaer. O, Gogus, Yalcin., Comparative study of irreversibilities in an aqua-ammonia absorption refrigeration system, *International Journal of Refrigeration*, Vol.14, (1991), pp. 86-92
5. Oh, M.D., Kim, S.C., Kim, Y.I., and Kim, Y.I., Cycle analysis of an air cooled LiBr/H₂O absorption heat pump of parallel flow type, *International Journal of Refrigeration*, Vol. 17, (1994), pp. 555-565
6. Aphornratana, S., Eames, I.W., Thermodynamic analysis of absorption refrigeration cycles using second law of thermodynamics method, *International Journal of Refrigeration*, Vol. 18(4), (1995), pp. 244-252
7. Bell, I.A., Al-Daini, A.J., Al-Ali, Habib., Abdel-Gayed, R.G., and Duckers, I., The design of an evaporator/absorber and thermodynamic analysis of a vapour absorption chiller driven by solar energy, *World Renewable Energy Congress*, (1996), pp. 657-660
- 53
8. Horuz, I., A comparison between ammonia-water and water lithium bromide solutions in vapour absorption refrigeration systems, *Heat and Mass Transfer*, Vol. 25(5), (1998), pp. 711-721
9. Ravikumar, T.S., Suganthi, L., and Anand, A.Samuel., Exergy analysis of solar assisted double effect absorption refrigeration system, *Renewable Energy*, Vol. 14(1-4), (1998), pp. 55-
10. Talbi, M.M., and Agnew, B., Exergy analysis: an absorption refrigerator using lithium bromide and water as the working fluids, *Applied Thermal Engineering*, Vol.20, (2000), pp. 619-
11. Lee, S.F., Sherif, S.A., Thermodynamic analysis of a lithium bromide/water absorption system for cooling and heating applications, *International Journal of Energy Research*, Vol.25, (2000), pp.1019-1031